A new mouse model of elastin haploinsufficiency highlights the importance of elastin to vascular development and blood pressure regulation

Bridget M. Brengle [1], Michelle Lin [1], Robyn A. Roth [1], Kara D. Jones [1], Jessica E. Wagenseil [2], Robert P. Mecham [3] and Carmen M. Halabi [1]

*1 - **Department of Pediatrics, Division of Nephrology,** Washington University School of Medicine, St. Louis, MO, USA*
*2 - **Department of Mechanical Engineering and Materials Science,** Washington University in St. Louis, St. Louis, MO, USA*
*3 - **Department of Cell Biology and Physiology,** Washington University School of Medicine, St. Louis, MO, USA*

***Corresponding author at:** 660 South Euclid Ave, Campus Box 8116, Saint Louis, MO, 63110. chalabi@wustl.edu.*
https://doi.org/10.1016/j.matbio.2023.02.003

Abstract

Supravalvular aortic stenosis (SVAS) is an autosomal dominant disease resulting from elastin (*ELN*) haploinsufficiency. Individuals with SVAS typically develop a thickened arterial media with an increased number of elastic lamellae and smooth muscle cell (SMC) layers and stenosis superior to the aortic valve. A mouse model of SVAS ($Eln^{+/-}$) was generated that recapitulates many aspects of the human disease, including increased medial SMC layers and elastic lamellae, large artery stiffness, and hypertension. The vascular changes in these mice were thought to be responsible for the hypertension phenotype. However, a renin gene (*Ren*) duplication in the original 129/Sv genetic background and carried through numerous strain backcrosses raised the possibility of renin-mediated effects on blood pressure. To exclude excess renin activity as a disease modifier, we utilized the Cre-LoxP system to rederive *Eln* hemizygous mice on a pure C57BL/6 background ($Sox2\text{-}Cre;Eln^{f/f}$). Here we show that $Sox2\text{-}Cre;Eln^{+/f}$ mice, with a single *Ren1* gene and normal renin levels, phenocopy the original global knockout line. Characteristic traits include an increased number of elastic lamellae and SMC layers, stiff elastic arteries, and systolic hypertension with widened pulse pressure. Importantly, small resistance arteries of $Sox2\text{-}Cre;Eln^{+/f}$ mice exhibit a significant change in endothelial cell function and hypercontractility to angiotensin II, findings that point to pathway-specific alterations in resistance arteries that contribute to the hypertensive phenotype. These data confirm that the cardiovascular changes, particularly systolic hypertension, seen in $Eln^{+/-}$ mice are due to *Eln* hemizygosity rather than *Ren* duplication.

Introduction

A closed circulatory system necessitates a strong yet flexible extracellular matrix (ECM) to withstand the energy produced during each cardiac cycle and allow continuous distal tissue perfusion. In large arteries, the protein elastin (ELN) confers the elastic recoil necessary for the aorta to store energy during systole and release it during diastole, dampening the pulse pressure generated by each heartbeat [1,2]. In the vasculature, ELN is organized in concentric sheets, known as lamellae, and the number of lamellae correlates directly with the tensional force in the wall [3]. The importance of intact elastin in vessel wall integrity is best surmised from diseases where elastin is either abnormally assembled, resulting in elastin fragmentation, or insufficiently produced, leading to reduced amounts of elastin in the arterial wall. Diseases with arterial elastic fiber fragmentation occur in individuals with mutations in fibrillin-1, lysyl oxidase and fibulin-4, which lead to Marfan syndrome [4,5], familial thoracic aortic aneurysm and dissection [6,7], and autosomal recessive cutis laxa type 1B [8–10], respectively. All share

ascending aortic aneurysms as a characteristic feature. In contrast, mutations resulting in *ELN* haploinsufficiency lead to supravalvular aortic stenosis (SVAS, OMIM #185500), which has vascular wall thickening and narrowing as a feature [11–13].

Williams-Beuren Syndrome (WBS, OMIM #194050) is a multisystem disorder that affects approximately 1/7,500 births and results from a 1.5Mb deletion of chromosome 7 that encompasses 25-27 genes, including *ELN* [14–16]. In addition to cardiovascular abnormalities, patients with WBS have intellectual disabilities, distinctive facial features, connective tissue abnormalities, growth abnormalities, and a gregarious personality [12,17]. Loss of *ELN* is responsible for the cardiovascular features of the syndrome, which vary in prevalence but include SVAS, arterial stenoses and hypertension. While commonly associated with WBS, SVAS also occurs as a non-syndromic autosomal dominant disease resulting from mutations in *ELN* [18,19]. Individuals with SVAS suffer from a thickened arterial media leading to narrowing of the arteries and an increased number of elastic lamellae and stenosis superior to the aortic valve. In contrast, the descending aorta, cerebral, and renal arteries remain normal [20–22]. Humans with SVAS also have increased vessel stiffness tested by pulse wave velocity and higher arterial blood pressure [21,23].

To study the consequences of elastin haploinsufficiency, mice lacking *Eln* ($Eln^{-/-}$) were generated using homologous recombination in the 129/Sv genetic background [24]. $Eln^{-/-}$ mice died between postnatal day (P) 0 and P4.5 due to the inward proliferation of medial SMCs resulting in obliteration of the vessel lumen. Like humans with SVAS, $Eln^{+/-}$ mice developed hypertension, an increased number of SMC layers and elastic lamellae despite reduced overall elastin content. Focal hourglass-like stenoses were absent, but diffuse stenosis was observed in most elastic vessels [25,26]. With repeated backcrossing to C57BL/6 mice, the blood pressure phenotype became less severe (~15% increase in systolic blood pressure over WT compared to the initially reported 36% increase) [27–30]. A genetic modifier screen to identify the source of blood pressure variability in these mice identified the renin gene as a candidate modifier [28]. Given that C57BL/6 mice contain one renin gene ($Ren\text{-}1^{c}$), while 129/Sv mice have two renin genes ($Ren\text{-}1^{d}$ and *Ren-2*) [31–33], there was concern that the hypertensive phenotype in $Eln^{+/-}$ mice was due to increased plasma renin levels and activation of the renin-angiotensin system [26] rather than a result of the vessel wall changes associated with elastin haploinsufficiency.

To address the relative contribution of vascular remodeling versus renin expression on cardiovascular hemodynamics and vessel function in $Eln^{+/-}$ mice, we utilized the Cre-LoxP system to generate a loss-of-function *Eln* mutation (*Sox2-Cre* crossed with a floxed elastin allele) in a pure C57BL/6 genetic background [34]. Herein we show that the cardiovascular abnormalities, particularly systolic hypertension, observed in $Eln^{+/-}$ mice are indeed due to elastin haploinsufficiency rather than renin gene duplication. Our results also rule out possible influences from the neomycin cassette that remains in the original knockout line.

Results

Complete loss of elastin leads to perinatal lethality

To eliminate the potential confounding effect of a mixed genetic background on the blood pressure phenotype in elastin haploinsufficiency, we regenerated a loss-of-function *Eln* allele on a pure C57BL/6 genetic background. *Sox2-Cre* mice (Jackson Laboratory, stock number: 008454) were crossed to previously described $Eln^{f/f}$ mice [34]. Early epiblast expression of Cre recombinase driven by the *Sox2* promoter allowed germline recombination, leading to an "excised" *Eln* allele (Eln^{ex}) in the gametes that were passed on to subsequent generations [35]. This eliminated the need for perpetual *Sox2-Cre* transgene transmission. While the $Eln^{+/ex}$ allele is a null allele that lacks exons 4 through 29, we refer to it as $Eln^{+/ex}$ in this report to distinguish it from the original knockout allele (Eln^{-}). $Eln^{+/ex}$ mice were born at the expected Mendelian ratios with no increase in mortality by six months of age. In contrast, $Eln^{ex/ex}$ mice did not survive past postnatal day (P) 0. At three months of age, there was no difference in body size between $Eln^{+/ex}$ mice and wild-type (WT) littermate control mice (Figure 1A). When examining the vasculature via visual inspection, no observable aneurysms or dilations were noted in any blood vessels. However, as previously reported [36], arterial elongation and tortuosity, particularly of the carotid artery, were seen in all $Eln^{+/ex}$ mice (Figure 1B).

Large arteries of $Eln^{+/ex}$ mice have an increased number of thinner elastic lamellae

When visualized by light microscopy using Alexa fluor 633 hydrazide staining of elastic fibers, the ascending aorta, descending thoracic aorta and carotid arteries of $Eln^{+/ex}$ mice had an increased number of elastic lamellae compared to WT vessels (Figures 2A&B). All lamellae, from adventitia to lumen, were found by transmission electron microscopy (TEM) to be ~50% thinner than those in WT littermate mice (Figures 2C&D). These lamellar number and thickness changes are similar to those documented for $Eln^{+/-}$ mice [25,26].

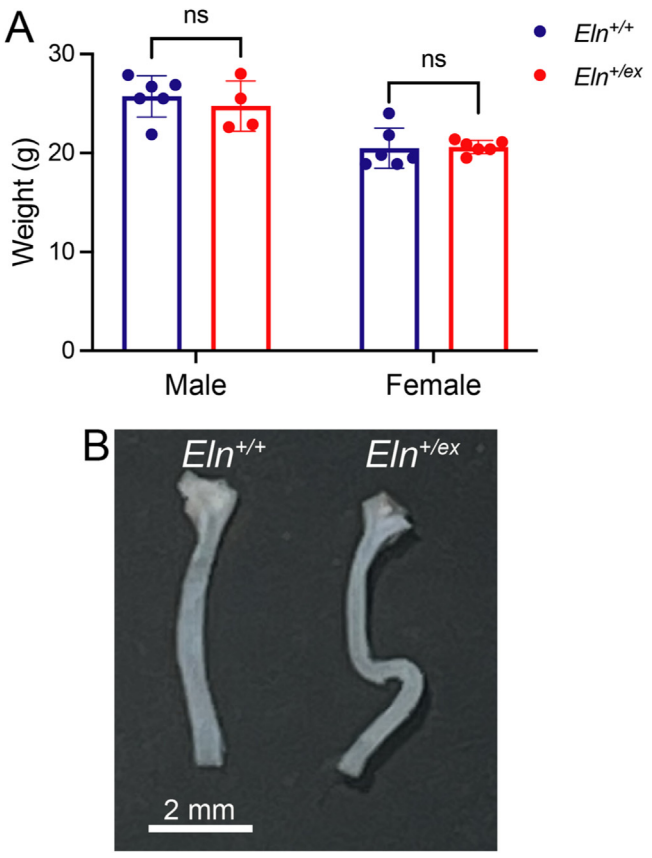

Figure 1. *Eln* hemizygosity does not affect body size, but leads to gross morphological changes in the vasculature. A) Body weight (in grams) of 3-4-month-old male and female $Eln^{+/ex}$ and littermate WT ($Eln^{+/+}$) mice. Data are presented as mean ± standard deviation. Two-way analysis of variance with Sidak's multiple comparisons test was performed to compare groups. ns = no statistically significant difference. B) Left common carotid artery dissected from its origin at the aortic arch (bottom) to its bifurcation (top) from $Eln^{+/+}$ and $Eln^{+/ex}$ mice. Elongation and tortuosity are noted in the mutant artery.

Elastin hemizygosity leads to increased large artery stiffness

Changes in ECM integrity often lead to changes in arterial mechanics. We tested the mechanical properties of $Eln^{+/ex}$ and $Eln^{+/+}$ large arteries by determining their pressure-diameter relationships. As seen in Figures 3A&C, the ascending aorta and carotid arteries of $Eln^{+/ex}$ mice reached maximum dilation at lower pressures than those of $Eln^{+/+}$ mice, indicating stiffer arteries. Importantly, at physiologic pressures, compliance of the $Eln^{+/ex}$ ascending aortae and carotid arteries, calculated as the change in diameter over the change in pressure, was significantly lower than that of WT littermates (Figures 3B&D).

$Eln^{+/ex}$ mice develop systolic hypertension that is unrelated to renin gene duplication

To assess the physiologic consequences of vessel wall changes and large artery stiffness, we measured central arterial blood pressure in $Eln^{+/ex}$ and WT littermate mice. As shown in Figures 4A, C, & D, and similar to $Eln^{+/-}$ mice [26], $Eln^{+/ex}$ mice had elevated systolic blood pressure, pulse pressure, and mean arterial pressure compared to WT littermate mice. Unlike $Eln^{+/-}$ mice, however, diastolic blood pressure and heart weight of $Eln^{+/ex}$ mice were not different than those of WT littermate mice (Figures 4B&F). The heart rate of $Eln^{+/ex}$ mice was similar to that of WT littermate mice (Figure 4E).

Due to concerns that hypertension in $Eln^{+/-}$ mice was due to *Ren* duplication, we developed a custom copy number assay to verify the number of renin genes in the $Eln^{+/ex}$ mice. The assay utilizes a primer/probe mix to amplify a genomic sequence common to all *Ren* genes (*Ren-1*^{c}, *Ren-1*^{d}, and *Ren-2*) (Figure 5A). A mouse with the C57BL/6 genetic background, which has a single copy of *Ren* (*Ren-1*^{c}), is expected to have two alleles, while a mouse with the 129/Sv genetic background, which has two copies of *Ren* (*Ren-1*^{d} and *Ren-2*), is expected to have four alleles. Genomic DNA from several $Eln^{+/ex}$ and $Eln^{+/+}$ mice, as well as from mice with the C57BL/6 and 129/Sv genetic

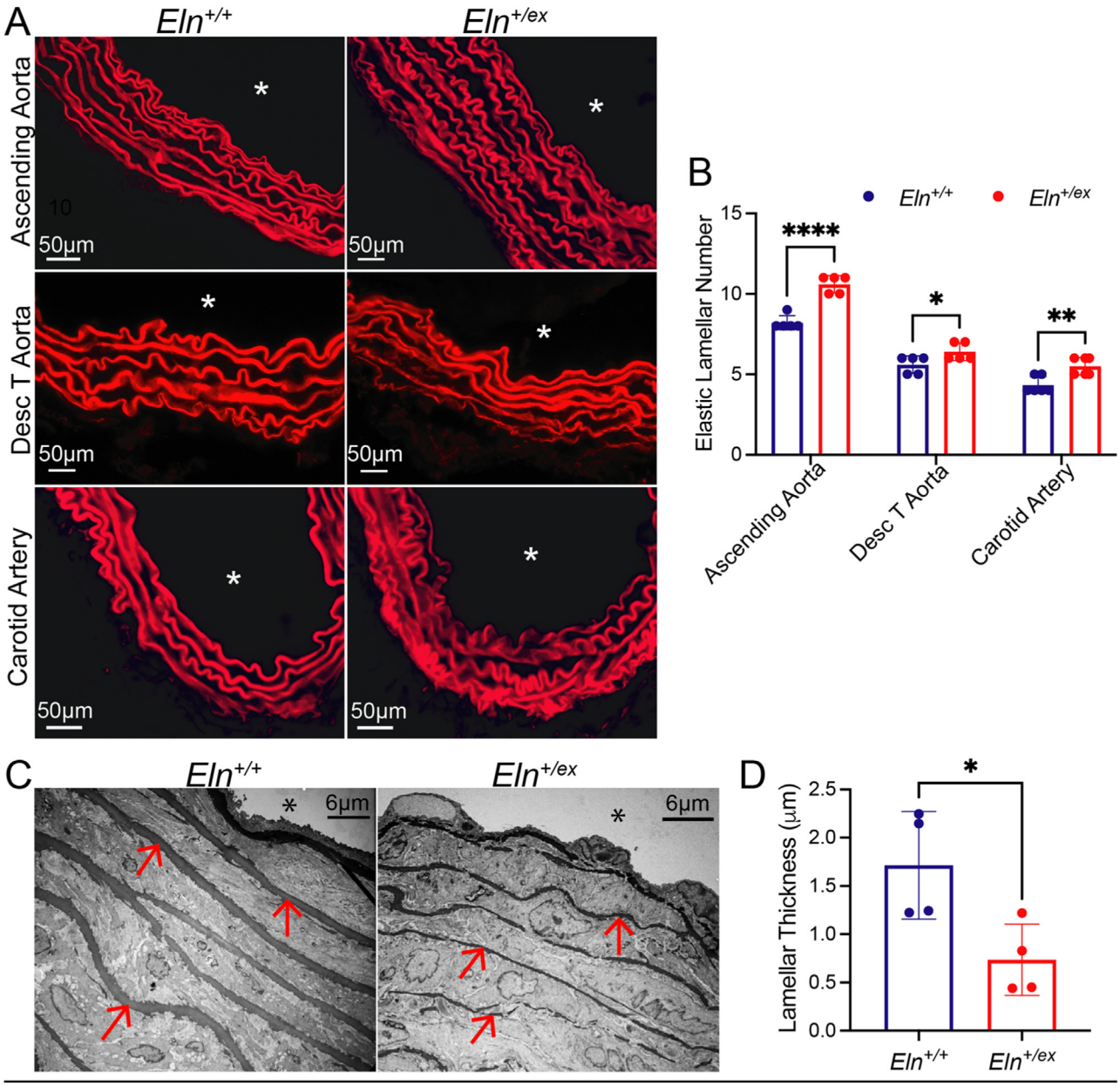

Figure 2. Arteries of *Eln*$^{+/ex}$ mice have an increased number of thinner elastic lamellae. A) Alexa Fluor 633 hydrazide staining of ascending aorta, descending aorta, and carotid arteries from 3-month-old *Eln*$^{+/ex}$ mice and WT (*Eln*$^{+/+}$) littermates. Elastic fibers appear in red. * indicates vessel lumen. B) Quantification of lamellar number in ascending aorta, descending thoracic aorta, and carotid arteries. C) Transmission electron micrographs of ascending aorta from *Eln*$^{+/+}$ and *Eln*$^{+/ex}$ mice. Red arrows indicate lamellae and * indicates vessel lumen. D) Quantification of elastic lamellar thickness taken as the average of three measurements from 3 different lamellae (9 total measurements) per mouse. Data are presented as mean ± standard deviation. Genotypes were compared using multiple unpaired student's t-tests. *P <0.05, **P <0.01, and ****P<0.0001.

backgrounds, was used to determine *Ren* copy number. As seen in Figure 5B, mice from the *Sox2-Cre;Eln*$^{+/f}$ colony (both *Eln*$^{+/ex}$ and *Eln*$^{+/+}$) and C57BL/6 mice had an average *Ren* copy number of 2, while 129/Sv mice had an average copy number of 4. To determine whether *Eln* haploinsufficiency affects renin gene expression or plasma renin levels, we assessed *Ren1* expression in the aorta and kidney of *Eln*$^{+/ex}$ and WT littermate mice. Plasma renin levels were determined in the same animals. As seen in Figures 5C&D, *Ren1* expression and plasma renin levels in *Eln*$^{+/ex}$ mice were similar to those of WT littermate mice. This is in contrast to the original *Eln*$^{+/-}$ mice, where plasma renin levels were more

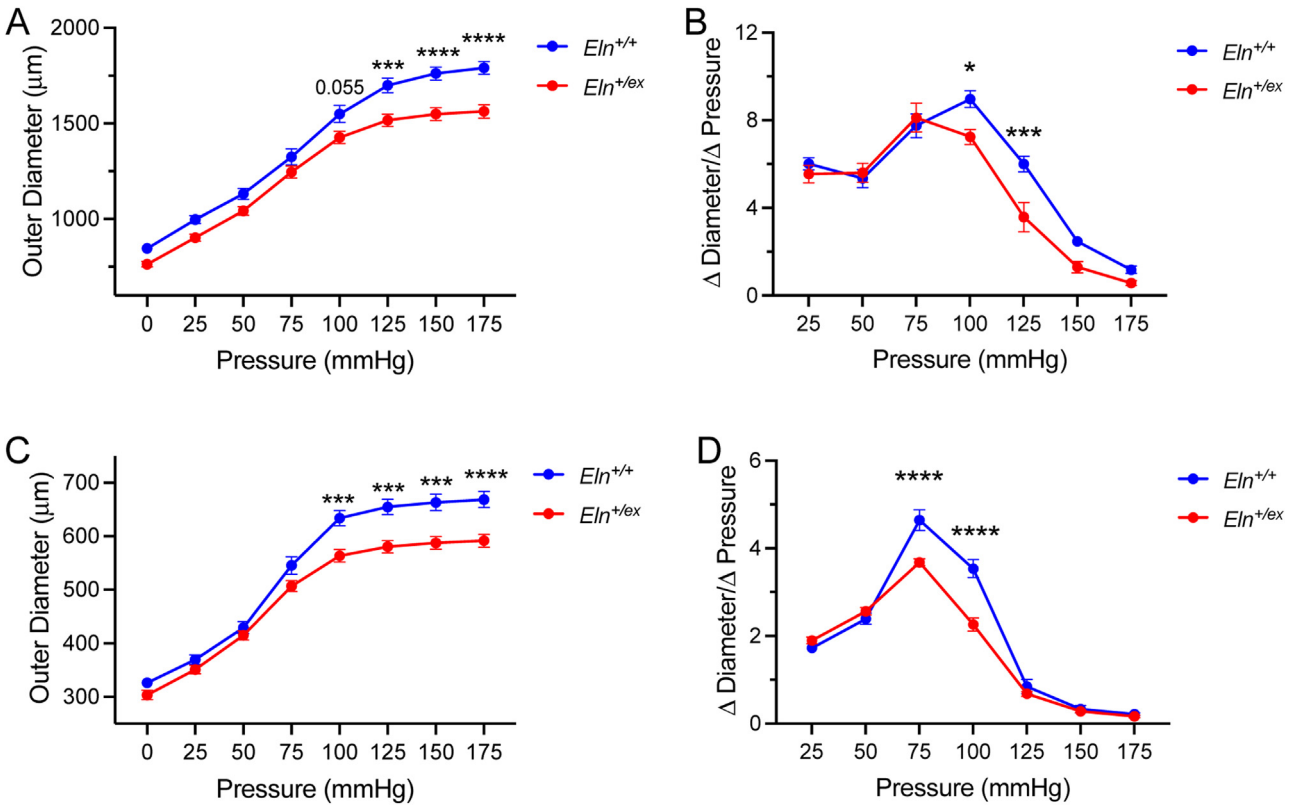

Figure 3. *Eln*$^{+/ex}$ mice exhibit increased large artery stiffness. (A&C) Pressure-diameter relationship of (A) ascending aorta and (C) left common carotid arteries from 3-month-old *Eln*$^{+/ex}$ and *Eln*$^{+/+}$ littermate mice. (B&D) Compliance of ascending aorta (B) and left common carotid arteries (D) of *Eln*$^{+/ex}$ and *Eln*$^{+/+}$ littermate mice calculated as change in diameter/change in pressure. Data are presented as mean ± standard error of the mean. Vessel diameter or change in diameter at each pressure was compared between genotypes using two-way ANOVA with Sidak's multiple comparisons test. n=6 for ascending aorta and 7 and 8 for carotid arteries of *Eln*$^{+/+}$ and *Eln*$^{+/ex}$, respectively. **P* <0.05, ****P* <0.001, *****P* <0.0001.

than twice those in WT animals [26]. Angiotensin II (angII) is the main effector of the renin-angiotensin system. We measured plasma angII concentrations and, as seen in Figure 5E, angII levels in *Eln*$^{+/ex}$ mice were similar to those of WT littermate mice.

Eln hemizygosity leads to changes in small vessel reactivity

Blood pressure is largely regulated by small resistance vessels, which were shown to have vascular bed-dependent abnormalities in reactivity in *Eln*$^{+/-}$ mice [37–39]. We examined the dilatory and contractile properties of *Eln*$^{+/ex}$ and *Eln*$^{+/+}$ third-order mesenteric arteries in response to various vasodilators and vasoconstrictors. As shown in Figures 6A&B, *Eln*$^{+/ex}$ mesenteric arteries had an impaired response to the endothelial-dependent vasodilator acetylcholine (Figure 6A) but not to the endothelium-independent vasodilator papaverine (Figure 6B), suggesting a significant change in endothelial cell function in *Eln*$^{+/ex}$ mesenteric arteries. The contractile ability of *Eln*$^{+/ex}$ mesenteric arteries was assessed using the vasoconstrictors phenylephrine (PE) and angII. As shown in Figures 6C&D, while their contractile response to PE was unaffected, *Eln*$^{+/ex}$ mesenteric arteries exhibited a hypercontractile response to angII at higher concentrations than WT vessels, similar to what was observed in *Eln*$^{+/-}$ mice [37,39].

Discussion

Studies of elastin haploinsufficiency (*Eln*$^{+/-}$) in humans and mice confirm that loss of one elastin allele has significant cardiovascular consequences. In particular, elastin haploinsufficiency leads to increased medial lamellar units, decreased elastin content, and increased stiffness of large arteries. It is important to note, however, that some of the cardiovascular phenotypes are not fully penetrant in humans and were found to have genetic modifiers in mice [11,23,25,26,28]. Hypertension, in particular, has an estimated prevalence of 40-50% in patients

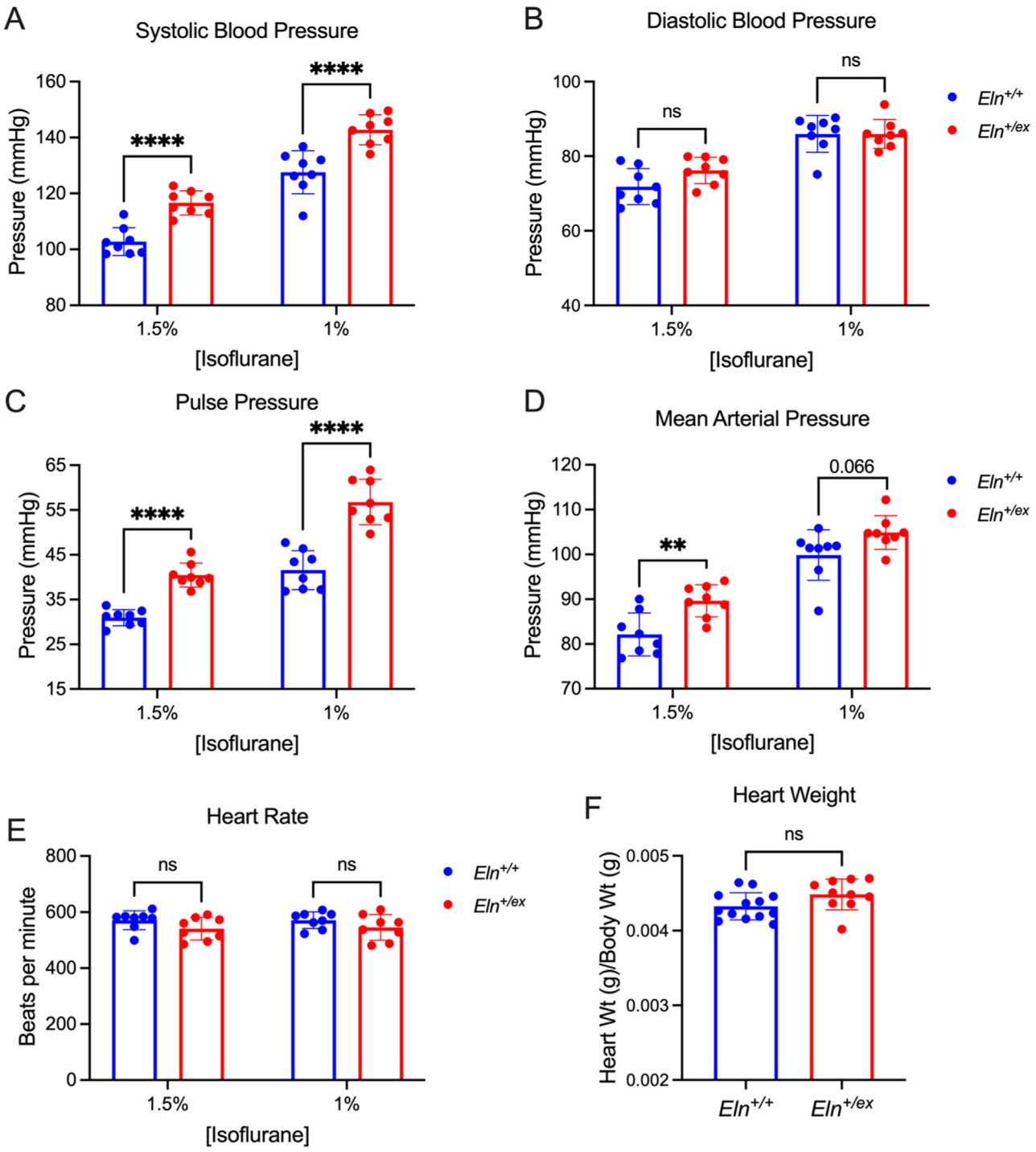

Figure 4. *Eln*$^{+/ex}$ mice exhibit systolic hypertension with widened pulse pressure without a change in heart rate or heart weight. Systolic blood pressure (A), diastolic blood pressure (B), pulse pressure (C), mean arterial pressure (D), heart rate (E) and heart weight to body weight ratios of 3-4-month-old *Eln*$^{+/ex}$ (red) and WT littermate (blue) male and female mice. Pulse pressure was calculated as the difference between systolic and diastolic blood pressure while mean arterial pressure was 2/3 diastolic +1/3 systolic blood pressure. Data are presented as mean ± standard deviation. Two-way ANOVA with Sidak's multiple comparisons test was used to compare differences between genotypes for all parameters except heart to body weight ratios, which were compared using student's unpaired t-test. **P<0.01, ***P <0.001, ****P<0.0001. ns = no statistically significant difference.

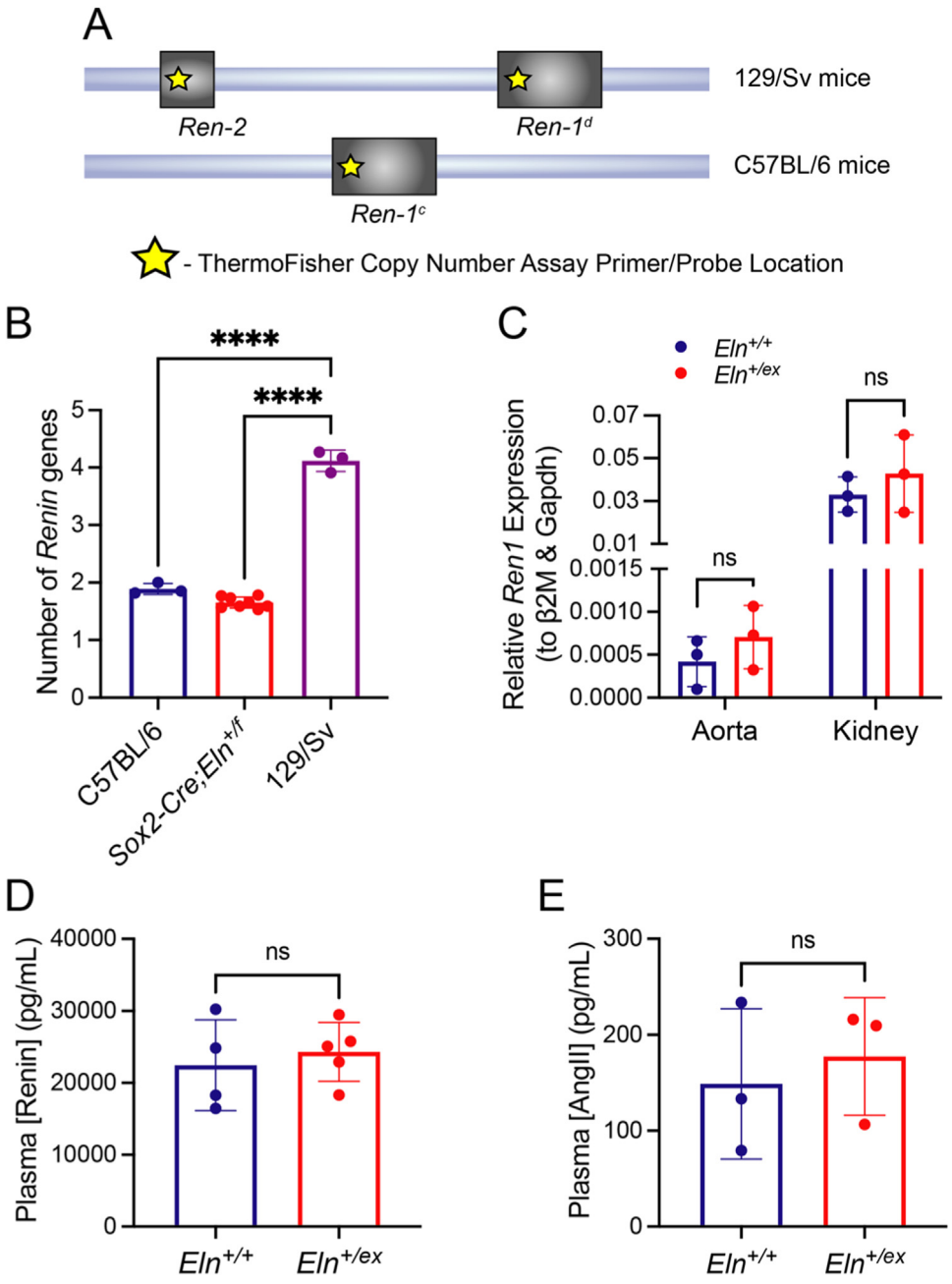

Figure 5. Mice generated from the *Sox2-Cre;Eln*$^{+/f}$ colony have a single copy of the renin gene and elastin haploinsufficiency does not affect renin or angiotensin II (AngII) levels. (A) Schematic representation of the custom-designed ThermoFisher renin gene (*Ren*) copy number assay. The yellow star indicates the area where the primer/probe was designed to amplify a genomic region common to all 3 renin genes. (B) Number of *Renin* genes in mice from the *Sox2-Cre;Eln*$^{+/f}$ line compared to mice with either C57BL/6 or 129/Sv genetic background as controls. C. qRT-PCR showing relative expression of *Ren1* in aorta and kidney of *Eln*$^{+/+}$ and *Eln*$^{+/ex}$ mice. D-E. Plasma renin (D) and AngII (E) concentrations in *Eln*$^{+/+}$ and *Eln*$^{+/ex}$ mice assessed using ELISA assays. Data are presented as mean ± standard deviation. One-way ANOVA with Dunnett's multiple comparisons test (B), two-way ANOVA with Sidak's multiple comparisons test (C), and unpaired t-test (D&E) were used to compare groups. ****P<0.0001.

with WBS [40–43], and, in mice, varies based on genetic background.

Eln$^{+/-}$ mice, originally generated in the 129/Sv genetic background and backcrossed to C57BL/6 mice, had an average increase of 36% and 21% in systolic and diastolic blood pressure, respectively, compared to WT mice (average BP 165/102 in *Eln*$^{+/-}$ mice vs. 121/84 in *Eln*$^{+/+}$ mice) [26]. Recently,

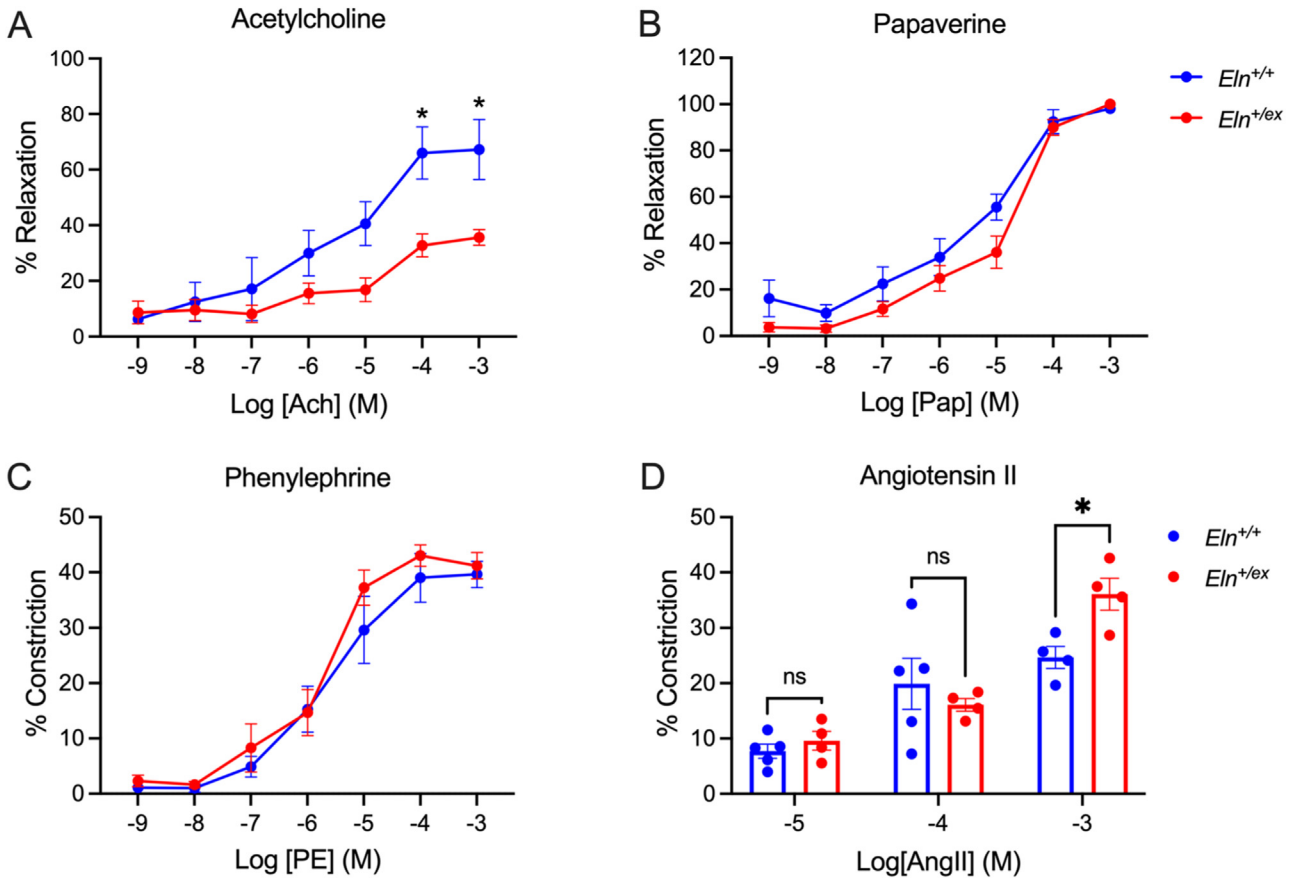

Figure 6. *Eln*$^{+/ex}$ hemizygosity leads to alterations in mesenteric artery reactivity. Dose-response relationships of third-order *Eln*$^{+/ex}$ (red) and *Eln*$^{+/+}$ (blue) mesenteric arteries assessing reactivity to acetylcholine (Ach) (A), papaverine (pap) (B), phenylephrine (PE) (C), and angiotensin II (AngII) (D). Data are presented as mean ± standard error of the mean. Two-way ANOVA with Sidak's multiple comparisons test was used to determine differences in vessel diameter between genotypes at each drug concentration. n=5 *Eln*$^{+/+}$, n=4 *Eln*$^{+/ex}$. *P <0.05.

however, reports using *Eln*$^{+/-}$ mice further backcrossed to the C57BL/6 genetic background found a ~15% increase in systolic blood pressure and no change in diastolic pressure compared to WT [27,29,30]. These hemodynamic changes, highly suggestive of physiological modifiers, prompted us to re-generate elastin haploinsufficient mice (*Eln*$^{+/ex}$) on a pure C57BL/6 background to investigate the potential effect of genetic background on the blood pressure phenotype. Table 1 summarizes the cardiovascular features of *Eln*$^{+/-}$ vs. *Eln*$^{+/ex}$ mice.

Global loss of elastin is incompatible with life, while its haploinsufficiency, as seen in humans with SVAS and in *Eln*$^{+/-}$ mice, leads to an increase in the number of thinner elastic lamellae and medial SMC layers that arise as a developmental adaptation to normalize vessel wall stress [24–26]. *Eln*$^{+/ex}$ mice recapitulate these vessel wall changes.

Blood pressure regulation is complex. Central to this process is the renin-angiotensin system, which regulates fluid and electrolyte balance and peripheral vascular resistance through the potent vasoconstrictor angII. The rate-limiting step in the generation of angII is the conversion of angiotensinogen to angiotensin I, which is catalyzed by the enzyme renin [44]. In humans and most experimental models, renin is synthesized as an inactive precursor, preprorenin, by the juxtaglomerular cells of the kidney from a single gene (*Ren-1*^{c}) [45]. In mice, however, the renin genes have variable copy number; some strains, such as the C57BL/6 strain, have the typical *Ren-1*^{c} while others, such as the 129/Sv strain, have two alternative genes at the renin locus, *Ren-1*^{d} and *Ren-2* [31–33]. In addition to having increased plasma renin levels, mice carrying two renin genes have elevated blood pressure (measured in both conscious and anesthetized mice) and cardiac weight index compared to those with one renin gene [44,46].

Quantitative trait locus analysis in *Eln*$^{+/-}$ mice identified the renin gene (*Ren1*) as a candidate modifier for hypertension [28]. *Eln*$^{+/-}$ mice generated in the 129/Sv background and backcrossed multiple times to C57BL/6 mice, had elevated systolic and

Table 1. Cardiovascular Characteristics of $Eln^{+/ex}$ vs. $Eln^{+/-}$ Mice.

		$Eln^{+/-}$	$Eln^{+/ex}$
Survival		↔	↔
Medial Lamellar Number	Ascending Aorta	↑	↑
	Descending Thoracic Aorta	↑	↑
	Carotid Artery	↑	↑
Elastic Lamellar Thickness		↓	↓
Arterial Blood Pressure	Systolic	↑↑	↑
	Diastolic	↑	↔
Heart Rate		↔	↔
Heart Weight		↑	↔
Plasma [Renin]		↑	↔
Large Artery Stiffness	Ascending Aorta	↑	↑
	Carotid Artery	↑	↑
Mesenteric Artery Reactivity			
Vasorelaxation	Acetylcholine	↓	↓
	Papaverine	↔	↔
Vasoconstriction	Angiotensin II	↑	↑
	Phenylephrine	↔	↔

↔ indicates unchanged compared to WT, ↑ indicates increased compared to WT and ↓ indicates decreased compared to WT. In red are differences between $Eln^{+/-}$ and $Eln^{+/ex}$ mice.

diastolic blood pressure as well as cardiac hypertrophy compared to WT mice. Furthermore, $Eln^{+/-}$ mice were shown to have elevated plasma renin levels compared to WT mice [26]. Our newly generated $Eln^{+/ex}$ mice on a pure C56BL/6 background, confirmed to have a single renin gene, have elevated systolic blood pressure, but exhibit no diastolic hypertension or cardiac hypertrophy compared to WT littermates. Furthermore, *Ren1* gene expression as well as plasma renin and angII levels in $Eln^{+/ex}$ mice were found to be similar to those of WT littermate mice. These data suggest that the elevated renin levels, likely due to the retention of two renin genes from the 129/Sv background, contribute to systolic hypertension (36% vs. 10%), diastolic hypertension and cardiac hypertrophy observed in the original $Eln^{+/-}$ mice [26].

While affected by large artery stiffness, blood pressure is mainly regulated by small resistance arteries, which account for most of the total peripheral vascular resistance [1,2]. Given the cross-talk between large and small arteries, several groups have examined the effect of large artery stiffness in elastin haploinsufficiency on resistance artery reactivity (responses to vasodilators and vasoconstrictors) in various vascular beds [37–39]. While mesenteric and cerebral arteries of $Eln^{+/-}$ mice display impaired endothelial-dependent vasodilation, endothelial function is preserved in skeletal muscle feed arteries. When vasoconstrictor responses were examined, mesenteric and cerebral arteries exhibited a hypercontractile response to angII but not to other vasoconstrictors such as norepinephrine, endothelin-1 and potassium chloride. In contrast, skeletal muscle feed arteries did not exhibit an altered response to any of the vasoconstrictors tested. Like $Eln^{+/-}$ mice, mesenteric arteries of $Eln^{+/ex}$ mice have an impaired response to acetylcholine but not papaverine, suggesting a significant change in endothelial cell function in these vessels. Based on studies done in $Eln^{+/-}$ mice, decreased nitric oxide bioavailability due to increased oxidative stress is likely the cause of this endothelial dysfunction [28,30,38], but that is yet to be explored in $Eln^{+/ex}$ mice. In addition to the significant change in endothelial cell function, $Eln^{+/ex}$ mesenteric arteries exhibit a hypercontractile response to angII, but not phenylephrine. These findings point to pathway-specific alterations in elastin haploinsufficient resistance arteries that

significantly contribute to the hypertensive phenotype. Indeed, angiotensin II type 2 receptor was recently shown to contribute to the systolic hypertension in *Eln*$^{+/-}$ mice [29].

In conclusion, by rederiving a mouse line hemizygous for elastin using a floxed-allele approach, we have generated a second model that confirms the essential effects of elastin on arterial development and vascular hemodynamics. This new line confirms the initial findings in the original knockout mouse that elastin haploinsufficiency leads to adaptive changes in vessel wall organization and arterial function. Inactivating *Eln* using a Crispr-generated floxed allele also excludes possible homologous recombination off-target effects, such as disruption of genes or regulatory elements near the elastin locus or the influence of the selection cassette in the targeting construct. Because the *Sox2-Cre;Eln*$^{f/f}$ line was generated in a pure C57BL/6 background containing a single renin gene and with normal renin levels, we can exclude a direct effect of renin on vessel wall remodeling. While changes in renin levels were a likely explanation for the decrease in blood pressure when the original knockout line was bred from the 129/Sv (2 renin genes) to the C57BL/6 (1 renin gene) background, elastin haploinsufficient mice with normal renin levels remain hypertensive. Stiffer elastic vessels associated with low elastin undoubtedly contribute to higher blood pressure. However, our finding of altered reactivity in muscular arteries brings the resistance vascular bed into focus as an underappreciated contributor to hypertensive disease in SVAS.

Experimental procedures

Mice and genotyping

Sox2-Cre mice were obtained from Jackson Laboratory (stock number: 008454) and *Eln*$^{f/f}$ mice were described elsewhere [34]. One male positive for Cre was bred to a female *Eln*$^{f/f}$ mouse. Germline transmission of the floxed allele was ensured by breeding one female *Sox2-Cre;Eln*$^{+/f}$ to a wildtype C57BL/6 male (Jackson Laboratory, stock number: 000664) and identifying Cre negative progeny carrying the excised elastin allele (*Eln*^{ex}). Removing the Sox2-Cre transgene allowed the propagation of *Eln*^{ex} without the perpetual need for Cre recombinase [35]. Male and female adult mice were used in all studies. All genotyping was confirmed through polymerase chain reaction genotyping using the following primer pairs: Cre forward, CGATGCAACGAGTGATGAGGT; Cre reverse, CCGACGATGAAGCATGTTTAGC (Cre positive, 255bp); Eln forward, CCATGTGGGTGCTGTAAGCT; Eln LoxP reverse, CCTACCTTTCTGGGGCCACT; Eln Excision reverse, GTGTGTGTAGCTGAGGAATGGG (Eln wildtype, 243bp; Eln LoxP, 283bp; Eln excised allele, 410bp). The mice were housed under standard conditions with free access to food and water with a twelve-hour light/dark cycle. All animal studies were approved by the Institutional Animal Care and Use Committee at Washington University in St. Louis.

Alexa 633 hydrazide staining and elastic lamellae counting

Ascending and descending thoracic aortas, and carotid arteries were dissected from adult mice, embedded in OCT compound, and frozen on dry ice. 5 μm-thick cryosections were placed on glass slides and stored at -80 °C until staining. Slides were fixed in 70% ethanol for 20 minutes at room temperature and washed with 1x phosphate buffered saline (PBS) twice (5 minutes each). The sections were then incubated in 1:1000 Alexa Fluor® 633 Hydrazide in 1x PBS for 5 minutes at room temperature and washed with 1x PBS twice (5 minutes each). The slides were mounted with ProLong Diamond Antifade Mountant with DAPI (Invitrogen) and imaged with a Zeiss Axiocam. Lamellae were counted manually using Image J software (NIH). The average lamellar count from two vessel sections was reported for each mouse. A minimum of 5 mice per genotype was analyzed.

Transmission electron microscopy

Eln$^{+/ex}$ and *Eln*$^{+/+}$ mice were sacrificed and vessels dissected after pressure fixation as previously described [47]. Briefly, after euthanasia and thoracotomy, the right atrium was clipped and 5 ml of 1x PBS was flushed through the left ventricle. 10% neutral buffered formalin (Fisher Scientific) was then allowed to flow through the left ventricle at 95-cm H_2O. Ascending aortas were dissected and fixed in 10% neutral buffered formalin at 4 °C for one week, then transferred to 2.5% glutaraldehyde (Electron Microscopy Sciences [EMS]) 4 °C for two to three weeks. Samples were washed with 1x PBS three times (20 minutes each) and fixed with 1.25% osmium tetroxide (EMS)/1x PBS for 1 hour at room temperature (RT) covered from light. After washing three more times in 1x PBS (20 minutes each), vessels were stained with 2% tannic acid (Sigma Aldrich) in 1x PBS for 1 hour. Samples were again washed three times in 1x PBS, followed by one wash in H_2O (15 minutes), two 15% ethanol/H_2O washes (15 minutes each), and one H_2O wash (30 minutes), then stained with 6% uranyl acetate (EMS)/H_2O for one hour in the dark. Excess stain was rinsed away with three washes of H_2O for 20 minutes each then the samples dehydrated through an ethanol series: 20% ethanol, 40% ethanol, 60%

ethanol, 80% ethanol, and 100% ethanol (20 minutes each). To ensure no water was left in the samples a total of five 100% ethanol exchanges (30 minutes each) were done and the samples rinsed twice in 100% propylene oxide (EMS) (20 minutes). The vessels were then infiltrated in 25% resin (Poly Sciences)/75% propylene oxide for 1 hour, 50% resin/50% propylene oxide for 1 hour, 75% resin/25% propylene oxide for 1 hour, and 100% resin overnight. Samples were embedded in fresh resin and left at RT for 8 hours, then at 60°C for 24 hours. Blocks were sectioned with an ultramicrotome at 60 nm thickness and collected on formvar coated slot grids, post stained with 6% uranyl acetate and lead citrate. Sections were imaged on a JEOL 1400 electron microscope and imaged with and AMT XR111 digital camera. Elastic lamellar thickness was then measured using ImageJ software (NIH). Three measurements of three different lamellae of the ascending aorta were averaged together for one mouse.

Arterial blood pressure and heart rate measurement

Central arterial blood pressure measurement was performed as previously reported [29]. Briefly, 3-4-month-old mice were anesthetized with 2% isoflurane, maintained at 37 °C and a Millar catheter (model SPR-1000) was introduced to the ascending aorta via the right common carotid artery. Once the surgical procedure was complete, recording was initiated using the PowerLab data acquisition system (ADInstruments) and isoflurane anesthesia was reduced to 1.5% for 5 min then to 1% for 5 min. The average of a 3-min period of stable recording was used to report systolic and diastolic blood pressure and heart rate. Data were analyzed using LabChart 8 for Mac software (ADInstruments).

Arterial pressure myography

Following blood pressure measurement and euthanasia, the ascending aorta and left common carotid arteries were dissected, cleaned of surrounding fat and maintained in physiological saline solution (PSS) composed of 130 mM NaCl, 4.7 mM KCl, 1.6 mM $CaCl_2$, 1.18 mM $MgSO_4$-$7H_2O$, 1.17 mM KH_2PO_4, 14.8 mM $NaHCO_3$, 5.5 mM dextrose, and 0.026 mM EDTA (pH 7.4) overnight at 4 °C. Arteries were then mounted on a pressure myograph (Danish Myo Technology), maintained in PSS at 37 °C and inflated from 0 to 175 mmHg in steps of 25 mmHg for 12 sec/step. Outer diameter of the vessel was visualized with an inverted microscope connected to a CCD camera and a computerized system and recorded at each step. The average of three measurements at each pressure was reported.

Copy number assay

We generated a custom TaqMan Copy Number Assay (Thermo Fisher) to determine the number of renin variants. Primer/probe sets were selected to amplify the first exons of *Ren1* and *Ren2* then run following manufacturer instructions. Briefly, 10 ng of genomic DNA was mixed with TaqMan Genotying MasterMix (2X, ThermoFisher Scientific, 4371353), TaqMan Copy Number Assay, TaqMan Copy Number Reference Assay Tfrc (20X, Thermo Fisher Scientific, 4458366), and water in a 96-well 0.1-mL plate. The real-time PCR was run using standard Applied Biosystems TaqMan Genotyping Assay. The CopyCaller software (Applied Biosystems) was used to analyze real-time PCR data using a Ct threshold of 0.2 and automatic baseline. Mice from the 129/Sv genetic background known to have two copies of renin and mice from the C57BL/6 genetic background known to have one renin copy were used as controls. The expected allele count was set to four for 129/Sv mice and two for C57BL/6 mice. *Sox2-Cre;Eln*$^{+/+}$ and *Sox2-Cre;Eln*$^{+/F}$ mice were both used in analysis.

Renin1 gene expression

Following euthanasia and thoracotomy, the right atrium was clipped and 5 ml of 1x PBS was flushed through the left ventricle. The thoracic aorta and half of the left kidney were dissected and placed RNA-Later at 4 °C until RNA was isolated using TRIzol following the manufacturer's protocol (Life Technologies). Following treatment with DNase I, 1 μg of RNA was used to generate cDNA in a 20 μL volume using High-Capacity RNA-to-cDNA kit according to manufacturer's protocol (Life Technologies). 1 μL of cDNA was then used along with TaqMan Fast Universal PCR Master Mix and TaqMan assays (primer/probes) to perform real-time PCR. Reactions were run in duplicate on the QuantStudio-3 real-time PCR system (Applied Biosystems). *Ren1* (Taqman assay Mm02342887_mH) gene expression was normalized to that of *Gapdh* (Mm99999915_g1) and β2-microglobulin (*B2m*, Mm00437762_m1).

Measurement of plasma renin and angiotensin II concentrations

Adult mice were exsanguinated under anesthesia and blood was collected in an EDTA-containing tube and placed immediately on ice. Samples were centrifuged at 500 x g for 15 min at 4 °C and the plasma collected was stored at -80 °C until ready for experimentation. Plasma was then used to measure either renin concentration using the Mouse Renin-1 ELISA Kit (Sigma, RAB0565) or angiotensin II concentration using the Angiotensin II EIA Kit (Sigma,

RAB0010) in duplicate. For the renin assay, plasma was diluted 1:2 using the diluent provided in the assay kit.

Small vessel reactivity

Following euthanasia, the gut from the duodenum to the cecum was excised and placed in cold normal Krebs' buffer (NB) containing: 120 mM NaCl, 25 mM $NaHCO_3$, 4.8 mM KCl, 1.2 mM NaH_2PO_4, 1.2 mM $MgSO_4$, 11 mM glucose and 1.8 mM $CaCl_2$ (pH 7.4). While maintained cold, third-order mesenteric arteries were excised, mounted on glass cannulas in the chamber of a pressure myography system (114P, Danish Myo Technology, Denmark) and tied in place with two pieces of nylon suture, as previously described [48]. Arteries were equilibrated at 37 °C for 30 min at 10 mmHg and initial responsiveness tested with 10 μM phenylephrine (PE) and 10 μM acetylcholine (Ach) at 60 mmHg. Vessels showing at least 40% dilation were used for subsequent experiments. To assess the vessels' dilation ability, vessels were pre-constricted with 10 μM PE and outer diameter measurements were collected after 1 min exposure to increasing Ach or papaverine concentrations [1×10^{-11}-1×10^{-3} μM] using the MyoVIEW 4 software. Increasing concentrations of PE [1×10^{-11}-1×10^{-3} μM] or angII [1×10^{-11}-1×10^{-5} μM] were used to measure constriction responses. The average of 2-3 vessels per drug was taken for each mouse, with 4-5 male and female mice per genotype. Acetylcholine chloride, papaverine, phenylephrine and human angiotensin II were purchased from Sigma-Aldrich (St. Louis, MO).

Data Availability

Data will be made available on request.

Declaration of Competing Interests

The authors declare no competing interests.

Acknowledgements

This work was supported by National Institutes of Health grants K08-HL 135400 to CMH, R01-HL53325 to RPM, and R56-HL152420 to JEW. Funds were also provided by the Ines Mandl Research Foundation to RPM.

Received 11 October 2022;
Received in revised form 9 January 2023;
Accepted 7 February 2023
Available online 10 February 2023

Keywords:
Supravalvular aortic stenosis;
Elastin haploinsufficiency;
Hypertension;
Arterial stiffness;
Endothelial dysfunction

Abbreviations:
SVAS, supravalvular aortic stenosis; WBS, Williams-Beuren Syndrome; SMCs, smooth muscle cells; ECM, extracellular matrix; Eln, elastin, Ren, renin

References

[1] M. Briet, E.L. Schiffrin, Treatment of arterial remodeling in essential hypertension, Curr. Hypertens. Rep. 15 (1) (2013) 3–9.
[2] S. Laurent, P. Boutouyrie, The structural factor of hypertension: large and small artery alterations, Circ. Res. 116 (6) (2015) 1007–1021.
[3] J.M. Clark, S. Glagov, Transmural organization of the arterial media. The lamellar unit revisited, Arteriosclerosis 5 (1) (1985) 19–34.
[4] H.C. Dietz, G.R. Cutting, R.E. Pyeritz, C.L. Maslen, L.Y. Sakai, G.M. Corson, E.G. Puffenberger, A. Hamosh, E.J. Nanthakumar, S.M. Curristin, et al., Marfan syndrome caused by a recurrent de novo missense mutation in the fibrillin gene, Nature 352 (6333) (1991) 337–339.
[5] F. Ramirez, B. Lee, E. Vitale, Clinical and genetic associations in Marfan syndrome and related disorders, Mt. Sinai J. Med. 59 (4) (1992) 350–356.
[6] D.C. Guo, E.S. Regalado, L. Gong, X. Duan, R.L. Santos-Cortez, P. Arnaud, Z. Ren, B. Cai, E.M. Hostetler, R. Moran, D. Liang, A. Estrera, H.J. Safi, G. University of Washington Center for Mendelian, S.M. Leal, M.J. Bamshad, J. Shendure, D.A. Nickerson, G. Jondeau, C. Boileau, D.M. Milewicz, LOX Mutations Predispose to Thoracic Aortic Aneurysms and Dissections, Circ. Res. 118 (6) (2016) 928–934.
[7] V.S. Lee, C.M. Halabi, E.P. Hoffman, N. Carmichael, I. Leshchiner, C.G. Lian, A.J. Bierhals, D. Vuzman, M. Brigham Genomic, R.P. Mecham, N.Y. Frank, N.O. Stitziel, Loss of function mutation in LOX causes thoracic aortic aneurysm and dissection in humans, Proc. Nat. Acad. Sci. U.S.A. 113 (31) (2016) 8759–8764.
[8] V. Hucthagowder, N. Sausgruber, K.H. Kim, B. Angle, L.Y. Marmorstein, Z. Urban, Fibulin-4: a novel gene for an autosomal recessive cutis laxa syndrome, Am. J. Hum. Genet. 78 (6) (2006) 1075–1080.
[9] M. Iascone, M.E. Sana, L. Pezzoli, P. Bianchi, D. Marchetti, G. Fasolini, Y. Sadou, A. Locatelli, F. Fabiani, G. Mangili, P. Ferrazzi, Extensive arterial tortuosity and severe aortic dilation in a newborn with an EFEMP2 mutation, Circulation 126 (23) (2012) 2764–2768.
[10] M. Kappanayil, S. Nampoothiri, R. Kannan, M. Renard, P. Coucke, F. Malfait, S. Menon, H.K. Ravindran, R. Kurup, M. Faiyaz-Ul-Haque, K. Kumar, A. De Paepe,

Characterization of a distinct lethal arteriopathy syndrome in twenty-two infants associated with an identical, novel mutation in FBLN4 gene, confirms fibulin-4 as a critical determinant of human vascular elastogenesis, Orphanet. J. Rare. Dis. 7 (2012) 61.
[11] L.M. Bird, G.F. Billman, R.V. Lacro, R.L. Spicer, L.K. Jariwala, H.E. Hoyme, R. Zamora-Salinas, C. Morris, D. Viskochil, M.J. Frikke, M.C. Jones, Sudden death in Williams syndrome: report of ten cases, J. Pediatr. 129 (6) (1996) 926–931.
[12] B.A. Kozel, B. Barak, C.A. Kim, C.B. Mervis, L.R. Osborne, M. Porter, B.R. Pober, Williams syndrome, Nat. Rev. Dis. Primers 7 (1) (2021) 42.
[13] J.C. Williams, B.G. Barratt-Boyes, J.B. Lowe, Supravalvular aortic stenosis, Circulation 24 (1961) 1311–1318.
[14] L.A. Perez Jurado, R. Peoples, P. Kaplan, B.C. Hamel, U. Francke, Molecular definition of the chromosome 7 deletion in Williams syndrome and parent-of-origin effects on growth, Am. J. Hum. Genet. 59 (4) (1996) 781–792.
[15] W.P. Robinson, J. Waslynka, F. Bernasconi, M. Wang, S. Clark, D. Kotzot, A. Schinzel, Delineation of 7q11.2 deletions associated with Williams-Beuren syndrome and mapping of a repetitive sequence to within and to either side of the common deletion, Genomics 34 (1) (1996) 17–23.
[16] P. Stromme, P.G. Bjornstad, K. Ramstad, Prevalence estimation of Williams syndrome, J. Child Neurol. 17 (4) (2002) 269–271.
[17] C.A. Morris, C.B. Mervis, Williams syndrome and related disorders, Annu. Rev. Genomics Hum. Genet. 1 (2000) 461–484.
[18] F. Chiarella, F.D. Bricarelli, G. Lupi, P. Bellotti, S. Domenicucci, C. Vecchio, Familial supravalvular aortic stenosis: a genetic study, J. Med. Genet. 26 (2) (1989) 86–92.
[19] M.L. Duque Lasio, B.A. Kozel, Elastin-driven genetic diseases, Matrix biology: journal of the International Society for Matrix Biology 71-72 (2018) 144–160.
[20] D.Y. Li, A.E. Toland, B.B. Boak, D.L. Atkinson, G.J. Ensing, C.A. Morris, M.T. Keating, Elastin point mutations cause an obstructive vascular disease, supravalvular aortic stenosis, Hum. Mol. Genet. 6 (7) (1997) 1021–1028.
[21] G. Merla, N. Brunetti-Pierri, P. Piccolo, L. Micale, M.N. Loviglio, Supravalvular aortic stenosis: elastin arteriopathy, Circulation. Cardiovascular genetics 5 (6) (2012) 692–696.
[22] K. Metcalfe, A.K. Rucka, L. Smoot, G. Hofstadler, G. Tuzler, P. McKeown, V. Siu, A. Rauch, J. Dean, N. Dennis, I. Ellis, W. Reardon, C. Cytrynbaum, L. Osborne, J.R. Yates, A.P. Read, D. Donnai, M. Tassabehji, Elastin: mutational spectrum in supravalvular aortic stenosis, European journal of human genetics: EJHG 8 (12) (2000) 955–963.
[23] B.A. Kozel, J.R. Danback, J.L. Waxler, R.H. Knutsen, L. de Las Fuentes, G.S. Reusz, E. Kis, A.B. Bhatt, B.R. Pober, Williams syndrome predisposes to vascular stiffness modified by antihypertensive use and copy number changes in NCF1, Hypertension 63 (1) (2014) 74–79.
[24] D.Y. Li, B. Brooke, E.C. Davis, R.P. Mecham, L.K. Sorensen, B.B. Boak, E. Eichwald, M.T. Keating, Elastin is an essential determinant of arterial morphogenesis, Nature 393 (6682) (1998) 276–280.
[25] D.Y. Li, G. Faury, D.G. Taylor, E.C. Davis, W.A. Boyle, R.P. Mecham, P. Stenzel, B. Boak, M.T. Keating, Novel arterial pathology in mice and humans hemizygous for elastin, J. Clin. Invest. 102 (10) (1998) 1783–1787.
[26] G. Faury, M. Pezet, R.H. Knutsen, W.A. Boyle, S.P. Heximer, S.E. McLean, R.K. Minkes, K.J. Blumer, A. Kovacs, D.P. Kelly, D.Y. Li, B. Starcher, R.P. Mecham, Developmental adaptation of the mouse cardiovascular system to elastin haploinsufficiency, J. Clin. Invest. 112 (9) (2003) 1419–1428.
[27] C.M. Halabi, T.J. Broekelmann, R.H. Knutsen, L. Ye, R.P. Mecham, B.A. Kozel, Chronic Antihypertensive Treatment Improves Pulse Pressure but Not Large Artery Mechanics in a Mouse Model of Congenital Vascular Stiffness, Am. J. Physiol. Heart Circ. Physiol. (2015) ajpheart 00288 2015.
[28] B.A. Kozel, R.H. Knutsen, L. Ye, C.H. Ciliberto, T.J. Broekelmann, R.P. Mecham, Genetic modifiers of cardiovascular phenotype caused by elastin haploinsufficiency act by extrinsic noncomplementation, J. Biol. Chem. 286 (52) (2011) 44926–44936.
[29] M. Lin, R.A. Roth, B.A. Kozel, R.P. Mecham, C.M. Halabi, Loss of Angiotensin II Type 2 Receptor Improves Blood Pressure in Elastin Insufficiency, Front Cardiovasc Med 8 (2021) 782138.
[30] A. Troia, R.H. Knutsen, C.M. Halabi, D. Malide, Z.X. Yu, A. Wardlaw-Pickett, E.K. Kronquist, K.M. Tsang, A. Kovacs, R.P. Mecham, B.A. Kozel, Inhibition of NOX1 Mitigates Blood Pressure Increases in Elastin Insufficiency, Function (Oxf) 2 (3) (2021) zqab015.
[31] D.P. Dickinson, K.W. Gross, N. Piccini, C.M. Wilson, Evolution and variation of renin genes in mice, Genetics 108 (3) (1984) 651–667.
[32] L.J. Field, K.W. Gross, Ren-1 and Ren-2 loci are expressed in mouse kidney, Proc. Nat. Acad. Sci. U.S.A. 82 (18) (1985) 6196–6200.
[33] C.D. Sigmund, K.W. Gross, Structure, expression, and regulation of the murine renin genes, Hypertension 18 (4) (1991) 446–457.
[34] C.J. Lin, M.C. Staiculescu, J.Z. Hawes, A.J. Cocciolone, B.M. Hunkins, R.A. Roth, C.Y. Lin, R.P. Mecham, J.E. Wagenseil, Heterogeneous Cellular Contributions to Elastic Laminae Formation in Arterial Wall Development, Circ. Res. 125 (11) (2019) 1006–1018.
[35] A.J. Song, R.D. Palmiter, Detecting and Avoiding Problems When Using the Cre-lox System, Trends Genet. 34 (5) (2018) 333–340.
[36] J.E. Wagenseil, N.L. Nerurkar, R.H. Knutsen, R.J. Okamoto, D.Y. Li, R.P. Mecham, Effects of elastin haploinsufficiency on the mechanical behavior of mouse arteries, Am. J. Physiol. Heart Circ. Physiol. 289 (3) (2005) H1209–H1217.
[37] P. Osei-Owusu, R.H. Knutsen, B.A. Kozel, H.H. Dietrich, K.J. Blumer, R.P. Mecham, Altered reactivity of resistance vasculature contributes to hypertension in elastin insufficiency, Am. J. Physiol. Heart Circ. Physiol. 306 (5) (2014) H654–H666.
[38] A.E. Walker, G.D. Henson, K.D. Reihl, R.G. Morgan, P.S. Dobson, E.I. Nielson, J. Ling, R.P. Mecham, D.Y. Li, L.A. Lesniewski, A.J. Donato, Greater impairments in cerebral artery compared with skeletal muscle feed artery endothelial function in a mouse model of increased large artery stiffness, J. Physiol. 593 (8) (2015) 1931–1943.
[39] A.E. Walker, E.K. Kronquist, K.T. Chinen, K.D. Reihl, D.Y. Li, L.A. Lesniewski, A.J. Donato, Cerebral and skeletal muscle feed artery vasoconstrictor responses in a mouse model with greater large elastic artery stiffness, Exp. Physiol. (2019).
[40] K. Bouchireb, O. Boyer, D. Bonnet, F. Brunelle, S. Decramer, G. Landthaler, A. Liutkus, P. Niaudet, R. Salomon, Clinical features and management of arterial hypertension in children with Williams-Beuren syndrome, Nephrology, dialysis, transplantation: official publication of the European Dialysis and

Transplant Association, European Renal Association 25 (2) (2010) 434–438.
[41] K. Broder, E. Reinhardt, J. Ahern, R. Lifton, W. Tamborlane, B. Pober, Elevated ambulatory blood pressure in 20 subjects with Williams syndrome, Am. J. Med. Genet. 83 (5) (1999) 356–360.
[42] M. Eronen, M. Peippo, A. Hiippala, M. Raatikka, M. Arvio, R. Johansson, M. Kahkonen, Cardiovascular manifestations in 75 patients with Williams syndrome, J. Med. Genet. 39 (8) (2002) 554–558.
[43] G.B. Ferrero, E. Biamino, L. Sorasio, E. Banaudi, L. Peruzzi, S. Forzano, L.V. di Cantogno, M.C. Silengo, Presenting phenotype and clinical evaluation in a cohort of 22 Williams-Beuren syndrome patients, European journal of medical genetics 50 (5) (2007) 327–337.
[44] C. Lum, E.G. Shesely, D.L. Potter, W.H. Beierwaltes, Cardiovascular and renal phenotype in mice with one or two renin genes, Hypertension 43 (1) (2004) 79–86.
[45] A.F. Clark, M.G. Sharp, S.D. Morley, S. Fleming, J. Peters, J.J. Mullins, Renin-1 is essential for normal renal juxtaglomerular cell granulation and macula densa morphology, J. Biol. Chem. 272 (29) (1997) 18185–18190.
[46] Q. Wang, E. Hummler, J. Nussberger, S. Clement, G. Gabbiani, H.R. Brunner, M. Burnier, Blood pressure, cardiac, and renal responses to salt and deoxycorticosterone acetate in mice: role of Renin genes, J. Am. Soc. Nephrol. 13 (6) (2002) 1509–1516.
[47] C.M. Halabi, T.J. Broekelmann, M. Lin, V.S. Lee, M.L. Chu, R.P. Mecham, Fibulin-4 is essential for maintaining arterial wall integrity in conduit but not muscular arteries, Sci. Adv. 3 (5) (2017) e1602532.
[48] S.R. Turner, M. Chappellaz, B. Popowich, A.A. Wooldridge, T.A.J. Haystead, W.C. Cole, J.A. MacDonald, Smoothelin-like 1 deletion enhances myogenic reactivity of mesenteric arteries with alterations in PKC and myosin phosphatase signaling, Sci. Rep. 9 (1) (2019) 481.